CONF-940285--1

SAND93-2557C

Axial Focusing of Impact Energy in the Earth's Interior: a Possible Link to Flood Basalts and Hotspots

M. B. BOSLOUGH, E. P. CHAEL, T. G. TRUCANO, D. A. CRAWFORD, and D. L. CAMPBELL

Sandia National Laboratories
Albuquerque, New Mexico 87123-0821, USA

Proceedings of the Conference on New Developments Regarding the KT Event and Other Catastrophes in Earth History

G. Ryder, S. Gartner, and D. Fastovsky, eds.

Geological Society of America Special Paper.

Axial Focusing of Impact Energy in the Earth's Interior: a Possible Link to Flood Basalts and Hotspots*

M. B. BOSLOUGH, E. P. CHAEL, T. G. TRUCANO,
D. A. CRAWFORD, and D. L. CAMPBELL

ABSTRACT

We present the results of shock physics and seismological computational simulations that show how energy from a large impact can be coupled to the interior of the Earth. The radially-diverging shock wave generated by the impact decays to linearly elastic seismic waves. These waves reconverge (minus attenuation) along the axis of symmetry between the impact and its antipode. The locations that experience the most strain cycles with the largest amplitudes will dissipate the most energy and have the largest increases in temperature (for a given attenuation efficiency). We have shown that the locus of maximum energy deposition in the mantle lies along the impact axis. Moreover, the most intense focusing is within the asthenosphere at the antipode, within the range of depths where mechanical energy is most readily converted to heat. We propose that if large impacts on the Earth leave geological evidence anywhere other than the impact site itself, it will be at the antipode. We suggest that the most likely result of the focusing for a sufficiently large impact, consistent with features observed in the geological record, would be a flood basalt eruption at the antipode followed by hotspot volcanism. A direct prediction of this model would be the existence of undiscovered impact structures whose reconstructed locations would be antipodal to flood basalt provinces. One such structure would be in the Indian Ocean, associated with the Columbia River Basalts and Yellowstone; another would be a second K/T impact structure in the Pacific Ocean, associated with the Deccan Traps and Reunion.

*This work was conducted at Sandia National Laboratories under the auspices of the Department of Energy under contract DE-AC04-94AL85000 under the LDRD program.

INTRODUCTION

The most obvious evidence for hypervelocity impacts in the geological record are the craters that they leave on the solid surfaces of planets and satellites. It was the cratered face of the moon that led to the first serious hypothesis for the process of impact by G.K. Gilbert (1893). Since then, understanding of the effects of hypervelocity impacts has focused on cratering (e.g. Melosh, 1988). However, impact is now known to have had many roles beyond making craters. Examples include control of the interior and surface thermal states of the Earth as it grew by impact-accretion (e.g. Kaula, 1979; Ahrens, 1994), the origin of the moon by the collision of a Mars-sized object with the early Earth (e.g. Taylor, 1994), and the mass extinction at the Cretaceous-Tertiary boundary (Alvarez et al. 1980). Evidence for other impact-induced extinctions has been cited (McLaren and Goodfellow, 1990), and there has been increasing speculation that energetic collisions have been responsible for geological processess as varied as continental flood basalt eruptions, mantle plumes, continental rifting, and geomagnetic pole reversals.

The cratering record has largely been erased on the Earth due to resurfacing by plate tectonics, volcanism, glaciation, and weathering. However, comparison to the cratered lunar surface leads directly to the conclusion that the Earth has experienced hundreds of impacts leaving craters the size of Chicxulub or larger. The purpose of our computational simulations was to enable us to develop a physical model for how a large impact could have affected the internal state of the Earth, which may have left evidence that remains long after the impact structure on the surface has disappeared.

Most planetary impact modeling has been aimed at explaining phenomena that have already been observed, and for that reason it has not been a predictive science. A notable exception is the recent impact of comet Shoemaker-Levy 9 on Jupiter, which provided an unprecedented opportunity for modelers to develop hypotheses and use them make predictions that could be directly tested by observation. Our group was able to demonstrate the power of computational modeling by predicting the fireball and plume phenomena (Boslough et al, 1994a,b, Crawford et al, 1994) that were later observed by astronomers (e.g. Hammel et al, 1994). Models for features already present in the geological record are more difficult to validate because they are not predictive. By contrast, the model described in this paper is subject to validation, because it specifically predicts both age and location of as-yet undiscovered impact structures.

BACKGROUND

A cause-and-effect connection between impacts and various geophysical processes has been the subject of extensive discussion and speculation. One of the earliest suggestions came from Seyfert and Sirkin (1979), who proposed that impact-induced mantle plumes could be a mechanism for initiating the breakup of plates. Burek and Wanke (1988) listed correlations between known Cenozoic impacts and geomagnetic field reversals, unconformity ages, shifts in paleotemperatures, and tectonic episodes. They suggested that major impacts could generate shock-induced phase transitions in the upper mantle, disrupting a delicately-balanced stability down to the core-mantle boundary. Rampino and Stothers (1988) proposed a quasi-periodic correlation between mass extinctions and major continental flood basalt volcanism over the last 250 million years and attempted to explain it in terms of episodic showers of impacting comets. Possible connections between impacts and the internal dynamics of the Earth are suggested by correlations of the ages of tektites from strewn fields with geomagnetic field reversals (Glass, 1979), and by a reversal associated with sediments deposited immediately after the impact that formed the Ries Crater (Pohl, 1977).

A causal link between major impact events and global processes would probably require a significant change in the thermal state of the Earth's interior, presumably brought about by coupling of impact energy. One possible mechanism for such energy coupling from the surface to the deep interior would be through focusing due to axial symmetry (Figure 1). Antipodal focusing of surface and body waves from earthquakes is a well-known phenomenon (Gutenberg and Richter 1934) which has previously been exploited by seismologists in studies of the Earth's deep interior (Rial, 1979; Chael, 1983). Antipodal focusing from impacts on the Moon, Mercury, and icy satellites has also been invoked by planetary scientists to explain unusual surface features opposite some of the large impact structures on these bodies (Schultz and Gault, 1975; Watts et al., 1991). For example, "disrupted" terrains have been observed antipodal to the Caloris impact basin on Mercury and the Imbrium basin on the Moon (Melosh, 1989). An antipodal relationship between the Hellas impact basin and the Alba Patera volcanism on Mars was pointed out by Peterson (1978), who suggested cause-and-effect. Williams and Greeley (1994) have performed computational modeling to determine the degree of focusing on Mars, and have suggested that the convergence of seismic waves was intense enough to fracture the Martian crust and provide a conduit for basaltic eruptions. There have also been recent speculations that antipodal focusing of impact energy may lead to flood basalt and hotspot activity on Earth (Hagstrum and Turrin, 1991; Rampino and Caldeira, 1992). However, these suggestions did not attempt to define a mechanism that could be subjected to rigorous modeling.

We believe that there is sufficient evidence in the geological record to suggest a causal relationship between large impact events and episodes of basaltic volcanism. A reasonable hypothesis is that seismic energy is coupled to the Earth's interior by focusing on the axis due to the first-order symmetry of both the energy source and the structure of the Earth's interior. It should be noted that our hypothesis is fundamentally different than those proposed by many others (e.g. Green, 1972; Alt et al., 1988; Oberbeck et al., 1992; Negi. et al., 1993) which involve melting and excavation at the impact location. Problems with models of this type have been pointed out by Melosh (1989), Loper and McCartney (1990), and Loper (1991). We believe that ours is a viable hypothesis, because 1) it invokes only processes that are independently known to take place (impacts and axial focusing), 2) it is testable by rigorous computational modeling, and 3) it is potentially predictive, i.e. it provides a basis for predicting the existence of currently unknown impact structures at antipodal locations to known flood basalt eruptions. The computational simulations presented in this paper provide the initial proof-of-principle test of the hypothesis, and give guidance for future work.

COMPUTATIONAL SIMULATIONS

We use two different types of simulations to model the asteroid impact and resulting seismic disturbance in the Earth's interior (Figure 1). A single computational method cannot accurately be applied to this problem because of the wide range in spatial and temporal scales and in peak stresses experienced. For example, during the impact event, the physical processes are occurring at scales on the order of the 10-km diameter asteroid, and 0.1 seconds after contact the peak shock pressures are 6 Mbar. Much later, when the energy is being dissipated within the Earth, the peak stresses are in the 10 bar range, and the wave motion takes place within the 12,000-km diameter of the Earth. Since it is very difficult to represent both extremes computationally, we have divided the problem into two parts. First, we investigate the source region, where the stresses and strain rates are high, using the strong-shock hydrodynamics code CTH. Second, we perform a seismological simulation that yields synthetic seismograms for various locations within the Earth by summing normal modes. These simulations demonstrate that displacement and strain amplitudes at the surface of the Earth near the antipode are orders of magnitude larger than those over most of the rest of the Earth's surface, and that the seismic energy remains sharply focused down to the core-mantle boundary.

CTH, the multi-dimensional multi-material elastic-plastic Eulerian code, was developed at Sandia National Laboratories (McGlaun et al., 1990). We used it to investigate the source region of a 10-km diameter asteroid impacting at 20 km/s. We have completed two-dimensional axisymmetric simulations to determine the influence of asteroid shape upon its interaction with the Earth in the near field (to a depth of 50 km below the impact point). The Earth is modeled using an ANEOS equation of state (Thompson, 1989), which contains thermodynamically consistent solid/melt and liquid/vapor phase transitions. Within a few seconds after impact, major shape differences become difficult to distinguish (Figure 2), demonstrating that, to first order, such an impact can be simulated as a point source when modeling far-field effects of the impact. The results of these near-field shock physics simulations can be used to generate source functions for the seismological simulations that are more accurate than the point source approximations, which will in turn yield more accurate strain histories. We expect that the deviations from point source functions will become more important as larger impacts are investigated. In the future, we will also use 3-D computational simulations to investigate the effects of impact angle.

Seismological simulations were carried out to predict the global response to a hypervelocity impact by using a point source function, as suggested by the shock physics simulations. The coupling of energy from major impacts to the mantle by axial focusing of seismic waves is very different than for a giant earthquake which, in addition to having less energy, has an asymmetric focal mechanism and a larger area. Displacement, stress and strain time histories were modeled through the use of normal mode synthetics. Each of the Earth's normal modes contributes a decaying sinusoid to the particle motion at a point in the Earth. The contribution of an individual mode to the observed motion at some point is a complex function of the source mechanism and the locations of the source and observation point. For our synthetics, we used the elastic, spherically-symmetric Earth model 1066A of Gilbert and Dziewonski (1975), for which there are existing compilations of the eigenfrequencies and radial eigenfunctions. The attenuation profile of the PREM model (Preliminary Reference Earth Model, Dziewonski and Anderson, 1981) was used to calculate the Q value for each of the 1066A modes.

The impact source was modeled as a vertical point force applied at the Earth's surface as a delta function in time. Assuming the impactor had a diameter of 10 km and an average density of 3 gm/cm^3, and that it collided with Earth at 20 km/s, we estimated the source impulse to be 3×10^{24} dyne-sec. Because of the symmetry, the Earth's toroidal modes are not excited by a vertical point force, thus only spheroidal modes were included in the calculations. Our synthetics represent the sum of 3382 modes, all of 1066A's spheroidal modes with frequencies less than 0.022 Hz (or periods greater than 45 seconds).

We generated synthetic displacement, stress and strain signals at several locations in and on the Earth, and measured the peak amplitudes from each of the signals. Figure 3 compares the displacement histories at six different angular distances from the source. This figure demonstrates the effect of antipodal focusing. Moving away from the source, the amplitudes of the signals decrease. Approaching the antipode (angular distance = Δ = 180°), however, this trend reverses and there is a dramatic increase in amplitude as energy traveling along all azimuths from the source converges. Surface displacements at the antipode are more than an order of magnitude larger than over most of the Earth's surface. Figure 4 shows the peak strain registered on the surface as a function of distance from the source. In this figure one can see how sharply the energy is focused at the antipode. Note that the strain at the antipode reaches a level comparable to that only a few degrees away from the impact. In Figure 5, the vertical displacement histories over the entire surface of the Earth are imaged, as a function of time and distance from the point of impact. The various seismic phases, which travel at different speeds and have different arrival times, appear as diagonal streaks on this diagram. The same information can be presented in a somewhat more intuitive manner by using it to generate a movie of the surface displacements on a globe. We have generated such a movie, in which surface waves and body wave arrivals can be seen propagating away from the impact site and focusing at the antipode. Selected frames from this movie are shown in Figure 6.

Figure 7 shows the variation of peak displacement amplitude with depth beneath the antipode, from the surface to the core-mantle boundary (CMB). Similarly, Figures 8 and 9 present the variation of peak strain and peak stress, respectively, with depth. Figures 7-9 demonstrate that the largest motions along the antipodal axis occur in the upper mantle at a depth corresponding to the asthenosphere, where seismic energy is most strongly attenuated. These large amplitudes are due to the fundamental-mode Rayleigh surface waves. At greater depths the Rayleigh-wave contribution diminishes, and the body arrivals become relatively more prominent.

Though the peak amplitudes decrease substantially with depth beneath the antipode, the signals at any depth still represent focused arrivals, with amplitudes much larger than seen at similar depths away from the antipodal axis. Figure 10 shows the displacement and strain records for three different locations on the core-mantle boundary. Figure 10a displays the motions on the CMB directly beneath the impact. The direct arrival, with a spherically spreading wavefront, is notably weaker than later focused arrivals. At an angular distance of 90° on the CMB (Figure

10b), there is no focusing and the amplitudes remain small throughout the signal. Figure 10c shows the motions on the CMB beneath the impact's antipode. Comparing Figures 10a and 10c, one sees that the motions on the CMB are actually greater beneath the antipode than beneath the source location. To improve on the seismic modeling, we plan to expand the set of included modes in order to extend the synthetics to higher frequencies. The body wave arrivals in particular will be better modeled by using a larger bandwidth. The shock physics simulations will be used to constrain the input source model. Finally, we will estimate the degradation in the focusing on the antipodal axis due to the Earth's lateral heterogeneity.

IMPLICATIONS

The strong focusing of seismic energy along a radius of the Earth beneath the antipode, and in particular into the asthenosphere, support the hypothesis that impacts can trigger rapid basaltic eruptions at the antipode. Moreover, the fact that a thermal anomaly remains in the mantle to great depth beneath the antipode provides a potential mechanism for the generation of a long-lived hotspot that remains fixed to the deeper mantle as the lithospheric plates move over it. This impact-induced thermal anomaly would mimic the mantle plumes currently postulated to be the cause of rapid flood basalt eruptions followed by hotspot tracks.

The impact-produced antipodal flood basalt hypothesis is attractive because it is directly testable on the basis of specific predictions of features in the geological record that have not yet been discovered. One can postulate that there is more than one type of trigger for flood basalt eruptions--some are triggered by mantle plumes and others by impact--but such a duel explanation is not scientifically satisfying. An economy of assumptions would require that if one episode of flood basalt volcanism was triggered by an impact, then all were This logically must lead to the prediction of impact structures antipodal to all flood basalt provinces (at the time of their formation). Unfortunately, the points that were antipodal to the many flood basalts observed on Earth are now subducted. One notable exception is the relatively young Columbia River Basalt province of the U.S. Pacific Northwest. The existence of an impact structure in the Indian Ocean, approximately antipodal to the associated hotspot (Yellowstone), and of the correct age (17 million years) would be sufficient evidence to confirm the hypothesis.

The impact hypothesis is in some critical ways more satisfying than current plume models for flood basalts and hotspots (e.g. Richards et al., 1989). First, it invokes only processes that are known to take place already; specifically large impacts and axial focusing of seismic energy. The plume models require the assumption of an instability leading to their formation, but a detailed mechanism subject to rigorous modeling has not been put forth. Second, the impact hypothesis is directly testable as suggested above. The plume hypothesis, by contrast, is inherently untestable for reasons listed by Anderson et al. (1992).

The impact hypothesis also provides a possible link between the K/T impact event and Deccan volcanism in India. The apparent coincidence between the timing of the largest known impact event and the largest episode of volcanic activity since the end of the Paleozoic era has been noted by many. There is evidence that the Deccan basalts were erupting prior to the impact (e.g. Venkatesan et al., 1993), but the precise timing relative to the Cretaceous-Tertiary boundary is still the subject of some debate. The position of India relative to the Chicxulub impact structure at the time of impact precludes the possibility of a direct link; India was thousands of kilometers west of the antipode. The evidence of a basaltic eruption at the antipode of Chicxulub has been subducted. However, the possibility of a simultaneous impact in the Pacific Ocean is plausible. Multiple impacts are known to occur, and until recently the Manson impact structure in Iowa was considered as a candidate for a second impact that the K/T boundary in western North America seemed to suggest. Some of the suggested mechanisms, such as the splitting of a comet shortly before impact with the Earth (Shoemaker et al., 1993), or impact by a binary asteroid (Grieve, 1993) would be expected to lead to nearly simultaneous impacts on the same hemisphere on Earth. Indeed, a second K/T impact site in the Pacific has been independently suggested on the basis of spinel spherule populations in K/T boundary deposits in a core from a drill site in the Pacific Ocean (Robin et al, 1993). If the proposed impact structure is sought, the location suggested by our hypothesis would be at a site in the Pacific consistent with a tectonic reconstruction antipodal to India.

The currently known impact structures are all at least partially on exposed land. Oceanic impact structures are difficult to locate because of the lack of detailed topographic and geologic data on the ocean floor (Grieve, 1987). The hypothetical link between the locations of flood basalts and oceanic impact sites provides a possible clue for where to begin to search. If such a link were to be confirmed by their existence, it would also provide a strong constraint on plate-tectonic reconstructions independent of paleomagnetic data or a presumed fixed hotspot reference frame. Moreover, it would provide a direct probe of mantle convection by providing the initial conditions and locations of hotspots, so their drift could be independently determined.

CONCLUSIONS

Our simulations provide the proof-of-principle basis for a testable hypothesis: large impacts on Earth generate thermal anomalies in the mantle that can lead to flood basalts and associated hotspots. This model leads directly to predictions for the existence of undiscoverd impact structures, and their disocovery would be a confirmation of the hypothesis. We have shown that displacement and strain amplitudes at the surface near the antipode of a large impact event on the Earth are orders of magnitude larger than those over most of the rest of the Earth's surface. For an impact of the size that occurred 65 million years ago, the peak displacement at the antipode approached ten meters, exceeding the ground motion only a few hundred kilometers from the source. Peak strains fall off rapidly with depth, but remain sharply focused along the impact-antipodal axis down to the core-mantle boundary. The region in the mantle that experiences the strongest focusing is the asthenosphere at the antipode, where seismic energy is most easily converted to heat. Future work will couple the shock physics simulations of the source region directly to the seismological model and include simulations of oblique impacts and larger impacts. We will also apply a realistic dissipation model to determine the extent of the resulting thermal anomaly in the Earth's interior for impacts of various energies.

ACKNOWLEDGEMENTS

This work was conducted at Sandia National Laboratories under the auspices of the Department of Energy under contract DE-AC04-94AL85000 under the LDRD program.

REFERENCES

Ahrens, T.J., 1994, The origin of the Earth: Physics Today, August, p. 38-45.

Alt D., Sears, J.M., and Hyndman, D. W., 1988, Terrestrial maria: the origins of large basalt plateaus, hotspot tracks and spreading ridges: J. Geol., v. 96, p. 647-662.

Alvarez, L.W., Alvarez, W., Asaro, F. and Michel, H.V., 1980., Extraterrestrial cause of the Cretaceous/Tertiary extinction: Science, v. 208, 1095-1108.

Anderson, D.L., Zhang, Y., and Tanimoto, T., 1992, Plume heads, continental lithosphere, flood basalts and tomography, in Storey, B.C., Alabaster, T. and Pankhurst, R.J., eds., Magmatism and the Causes of Continental Break-up, Geological Society Special Publication No. 68, pp. 99-124.

Boslough, M.B., Crawford, D.A., Robinson, A.C., and Trucano, T.G., 1994a, Mass and penetration depth of Shoemaker-Levy 9 fragments from time-resolved photometry: Geophys. Res. Lett., v. 21, p. 1555-1558.

Boslough, M.B., Crawford, D.A., Robinson, A.C., and Trucano, T.G., 1994b, Watching for fireballs on Jupiter: EOS (American Geophysical Union Transactions),, v. 75, p.305-310.

Burek, P.J., and Wanke, H., 1988, Impacts and glacio-eustasy, plate-tectonic episodes, geomagnetic reversals: a concept to facilitate detection of impact events: Phys. Earth Planet. Inter., v. 50, p. 183-194.

Chael, E.P., 1983, Constraints on the Earth's anelastic and aspherical structure from antipodal surface waves [Ph.D. thesis]: California Institute of Technology, 139 pp.

Crawford, D.A., Boslough, M.B., Trucano, T.G., and Robinson, A.C., 1994, The impact of comet Shoemaker-Levy 9 on Jupiter: Shock Waves, v. 4, p. 47-50.

Dziewonski, A.M., and Anderson, D.L., 1981, Preliminary reference Earth model: Phys. Earth Planet. Inter., v. 25, p. 297-356

Gilbert, G.K., 1893, The moon's face: a study of the origin of its features: Bull. Phil. Soc. Wash., v. 12, p. 241-292.

Gilbert, F., and Dziewonski, A.M., 1975, An application of normal mode theory to the retrieval of structural parameters and source mechanisms from seismic spectra: Phil. Trans. Roy. Soc. Lond. A, v. 278, p. 187-269

Glass, B.P., Swincki, M.B., and Zwart, P.A., 1979, in Proceedings. Lunar Planetary Science Conference 10th, Pergamon, p. 25-37, .

Green, D.H., 1972, Archaen greenstone belts may include terrestrial equivalents of lunar maria?: Earth and Planet. Sci. Lett., v. 15, p. 263-270.

Grieve, R.A.F., 1987, Terrestrial impact structures: Annual Review of Earth and Planetary Sciences, v. 15, p. 245-270.

Grieve, R.A.F., 1993, When will enough be enough?: Nature, v. 363, p. 670-671.

Gutenberg, B., and Richter, C., 1934, Gerlands Beitr. Geophys., v. 43, p. 56.

Hagstrum, J.T., and Turrin, B.D., 1991, Is flood basalt volcanism a seismically-induced response to large antipodal bolide impacts? [abs.]: EOS (American Geophysical Union Transactions), v. 72, p. 516.

Hammel et al., 1994, xxx, Science (in press).

Kaula, W.M., 1979, Thermal evolution of Earth and Moon growing by planetesimal impacts: J. Geophys. Res., v. 84, p. 999-1008.

Loper, D.E., and McCartney, K., 1990, On impacts as a cause of geomagnetic field reversals or flood basalts. in Sharpton, V.L., and Ward, P.D., eds., Global catastrophes in Earth history; An interdisciplinary conference on impacts, volcanism, and mass mortality: Geological Society of America Special Paper 247.

Loper,D.E., 1991, Mantle plumes: Tectonophys., v. 187, p. 373-384.

McGlaun, J. M., Thompson, S. L., and Elrick, M. G., 1990, CTH: a three dimensional shock-wave physics code, Int. J.; Impact. Engng., v. 10, p. 351.

McLaren, D.J., and Goodfellow, W.D., 1990, Geological and biological consequences of giant impacts: Annual Review of Earth and Planetary Sciences, v. 18, p. 123-171.

Melosh, H.J., 1989, Impact cratering: a geologic process: New York, Oxford University Press, 245 p.

Negi, J.G., Agrawal, P.K., Pandey, O.P. and Singh, A.P., 1993, A possible K-T boundary bolide impact site offshore near bombay and triggering of rapid Deccan volcanism: Phys. Earth Planet. Int., v. 76, p. 189-197.

Oberbeck, V.R., Marshall, J.R., and Aggarwal, H., 1992, Impacts, tillites, and the breakup of Gondwanaland, J. Geol., v. 101, p. 1-19.

Peterson, J.E., 1978, Antipodal effects of major basin-forming impacts on Mars [abs.]: Lunar Planet. Sci. v9, p. 885-886.

Pohl, J., 1977, Paleomagnetische und gesteinsmagnetische untersuchungen an den kermen der Forschungsbohrung Noerdingen: Geol. Bavarica, v. 75, p. 329-348.

Rampino, M.R., and Strothers, R.B., 1988, Flood basalt volcanism during the past 250 million years: Science, v. 241, p. 663-668.

Rampino, M.R., and Caldeira, K., 1992, Antipodal hotspot pairs on the Earth: Geophys. Res. Lett., v. 19, p. 2011-2014.

Rial, J.A., 1979 Seismic waves at the epicenter's antipode, Part II [Ph.D. thesis]: California Institute of Technology, 117 pp.

Richards, M.A., Duncan, R.A., and Courtillot, V.E., 1989, Flood Basalts and hot-spot tracks: plume heads and tails: Science v. 246, p. 103-107.

Robin, E., Froget, L., Jehanno, C. and Rocchia, R., 1993, Evidence for a K/T impact event in the Pacific Ocean: Nature, v. 363, p. 615-617.

Schultz, P.H., and Gault, D.E., 1975, Seismic effects from major basin formation of the Moon and Mercury: The Moon, v. 12, pp. 159-177.

Shoemaker, E.M., Roddy, D.J., and Anderson, R.R., 1993, Research program on the Manson impact structure, Iowa [abs.]: Lunar Planet. Sci. v 24, p. 1301-1302.

Seyfert, C.K., and Sirkin, L.A., 1979, Earth history and plate tectonics: New York, Harper & Row.

Taylor, G.J., 1994, The scientific legacy of Apollo: Scientific American, July, p. 40-47.

Thompson, S. L., 1989, ANEOS analytic equations of state for shock physics codes input manual, Sandia National Laboratories, SAND89-2951.

Venkatesan, T.R., Pande, K., and Gopalan, K., 1993, Did Deccan volcanism pre-date the Cretaceous/Tertiary transition?: Earth and Planet. Sci. Lett., v. 119, p. 181-189.

Watts, A.W., Greeley, R., and Melosh, H.J., 1991, The formation of terrains antipodal to major impacts: Icarus, v. 93, p. 159-168.

Williams, D.A., and Greeley, R., 1994, Assessment of antipodal-impact terrains on Mars: Icarus, v. 110, p. 196-202.

Figure Captions

Figure 1. Cross-section of the Earth, showing why seismic energy focuses on the axis. The shock physics simulations are limited to the impact source region, and the seismological simulations are over the entire interior. Various families of compressional seismic rays are drawn.

Figure 2. Shock wave physics simulations of the source region of the impact of a 10-km diameter asteroid at 20 km/s onto the Earth.

Figure 3. Radial displacement histories on the Earth's surface at six different angular distances from the impact. The peak amplitude at the antipode approaches 10 meters, similar to what it is only 2° from the source.

Figure 4. Peak strain amplitudes as a function of radial distance from the impact source.

Figure 5. Image of vertical displacement at the Earth's surface as a function of time and distance from impact.

Figure 6. Selected frames from movie of seismic waves propagation away from impact site and focusing on the antipode (a) shortly after impact, (b) 45 minutes after impact, and (c) 87 minutes after impact. Vertical displacements are shown as height above globe, relative to maximum displacement at the time step shown. Continents are in their present locations, not at their positions at the time of impact.

Figure 7. Peak radial displacement amplitude as a function of depth beneath the antipode down to the core-mantle boundary (CMB).

Figure 8. Peak strain amplitude as a function of depth beneath the antipode down to the CMB.

Figure 9. Peak stresses amplitudes as a function of depth beneath the antipode down to the CMB.

Figure 10. Radial displacement and strain histories at three locations just above the CMB: (a) Beneath the impact source (Δ=0°). (b) Equidistant between the impact and antipode (Δ=90°). (c) Beneath the antipode (Δ=180°).

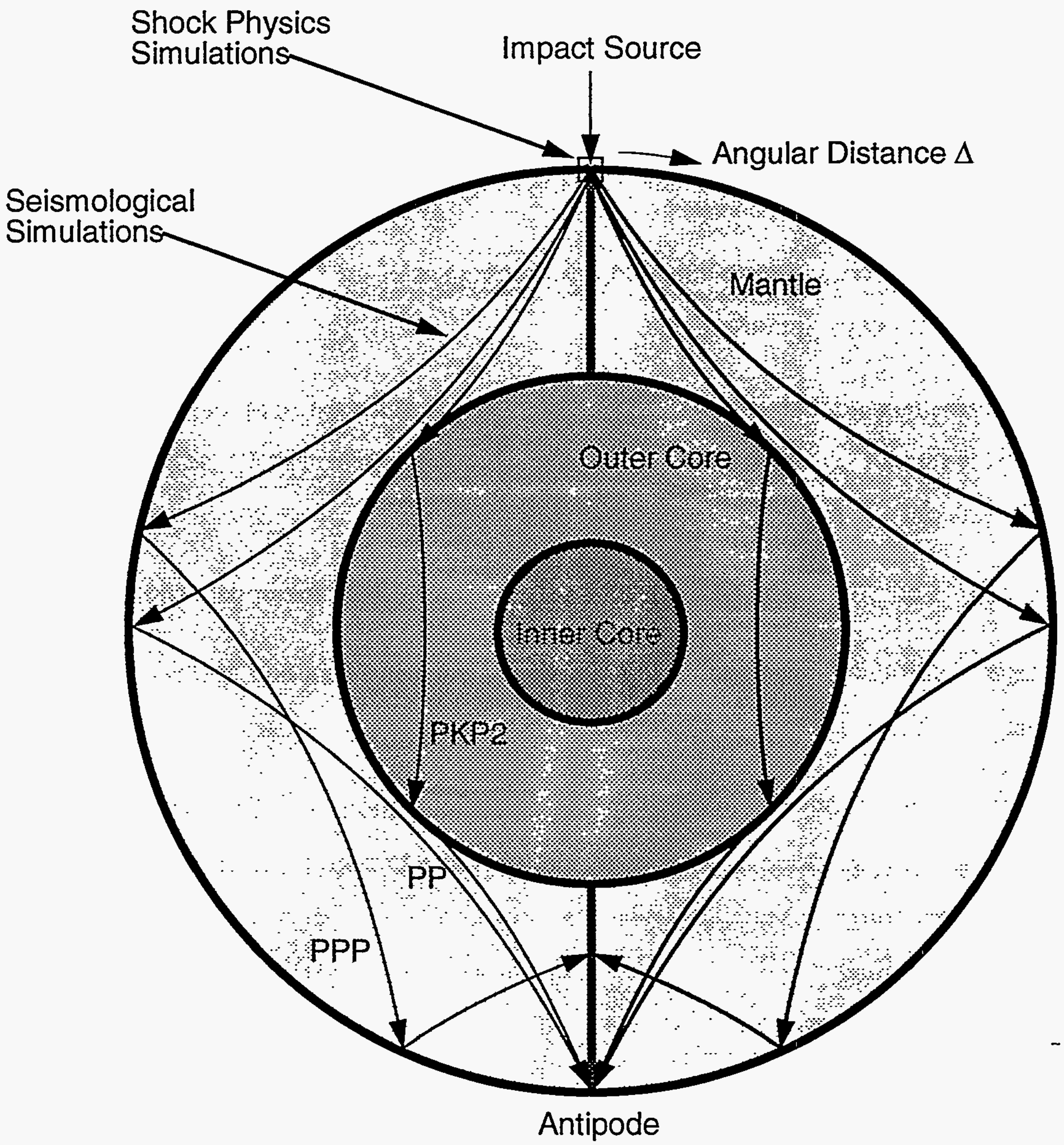
Shock Physics Simulations
Impact Source
Angular Distance Δ
Seismological Simulations
Mantle
Outer Core
Inner Core
PKP2
PP
PPP
Antipode

Figure 1

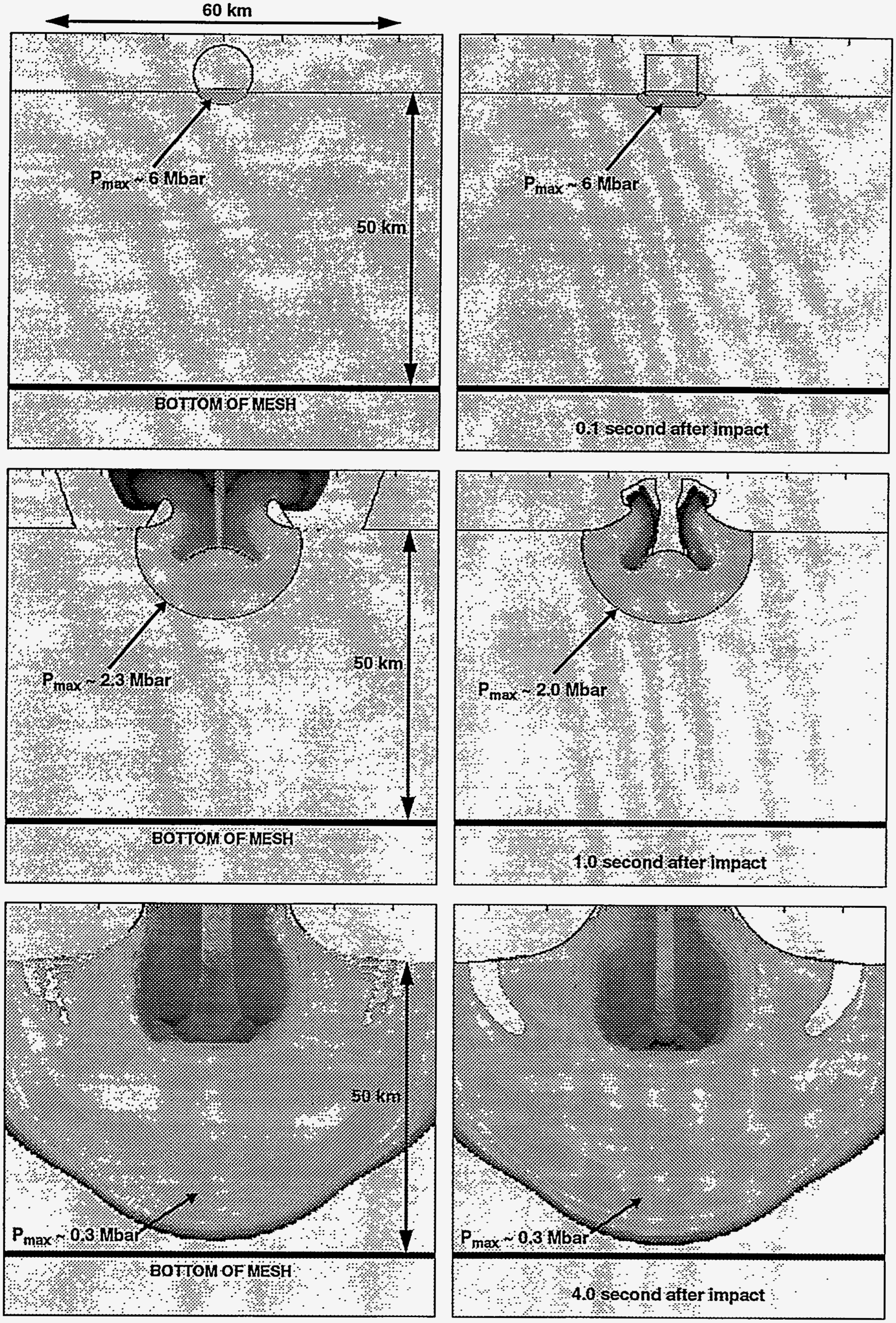

60 km
P max ~ 6 Mbar
50 km
BOTTOM OF MESH
P max ~ 6 Mbar
0.1 second after impact
P max ~ 2.3 Mbar
50 km
BOTTOM OF MESH
P max ~ 2.0 Mbar
1.0 second after impact
50 km
P max ~ 0.3 Mbar
BOTTOM OF MESH
P max ~ 0.3 Mbar
4.0 second after impact

Figure 2

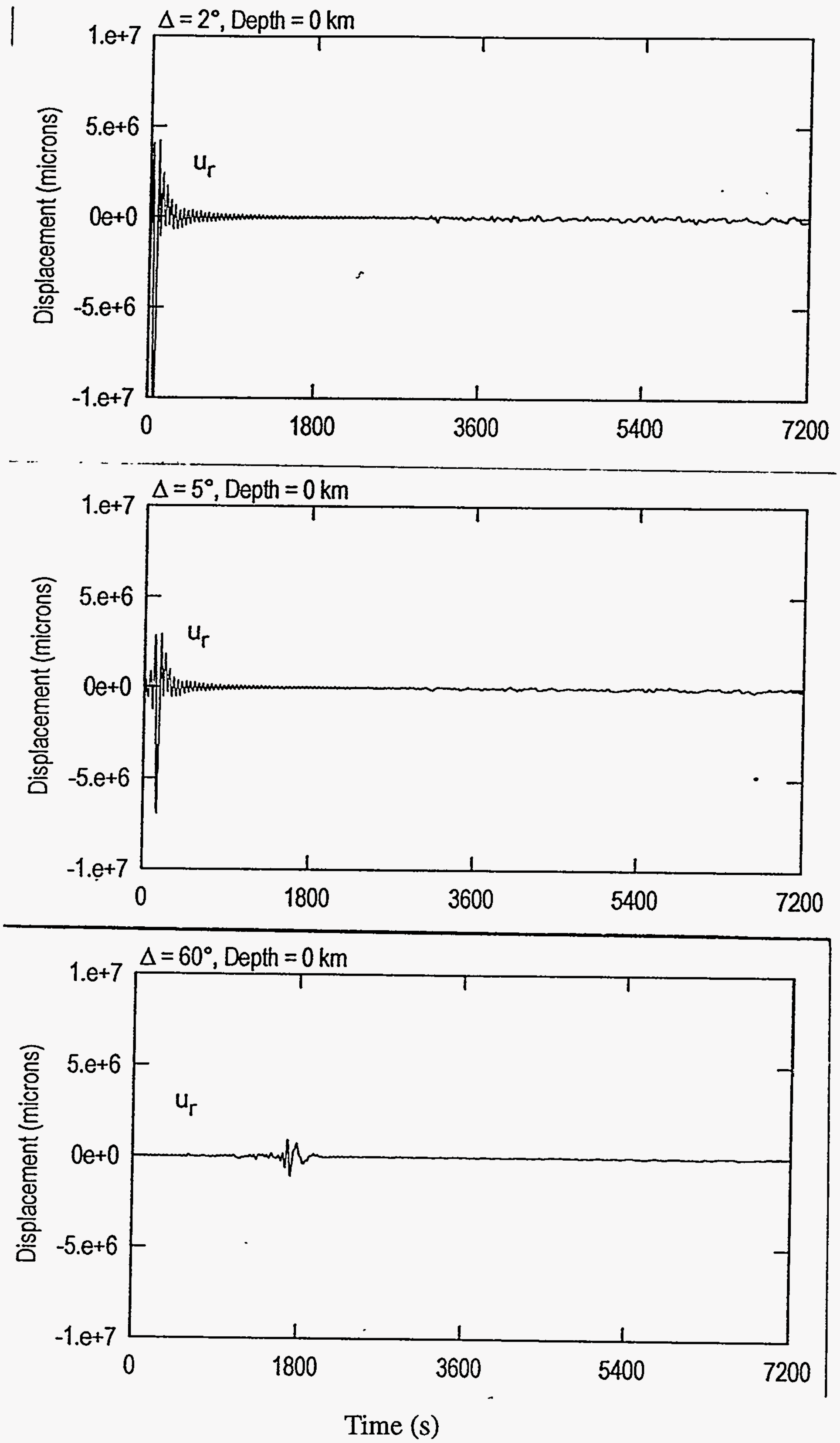

Δ = 2°, Depth = 0 km
Δ = 5°, Depth = 0 km
Δ = 60°, Depth = 0 km
Displacement (microns)
1.e+7
5.e+6
0e+0
-5.e+6
-1.e+7
u_r
0
1800
3600
5400
7200
Time (s)

Figure 3

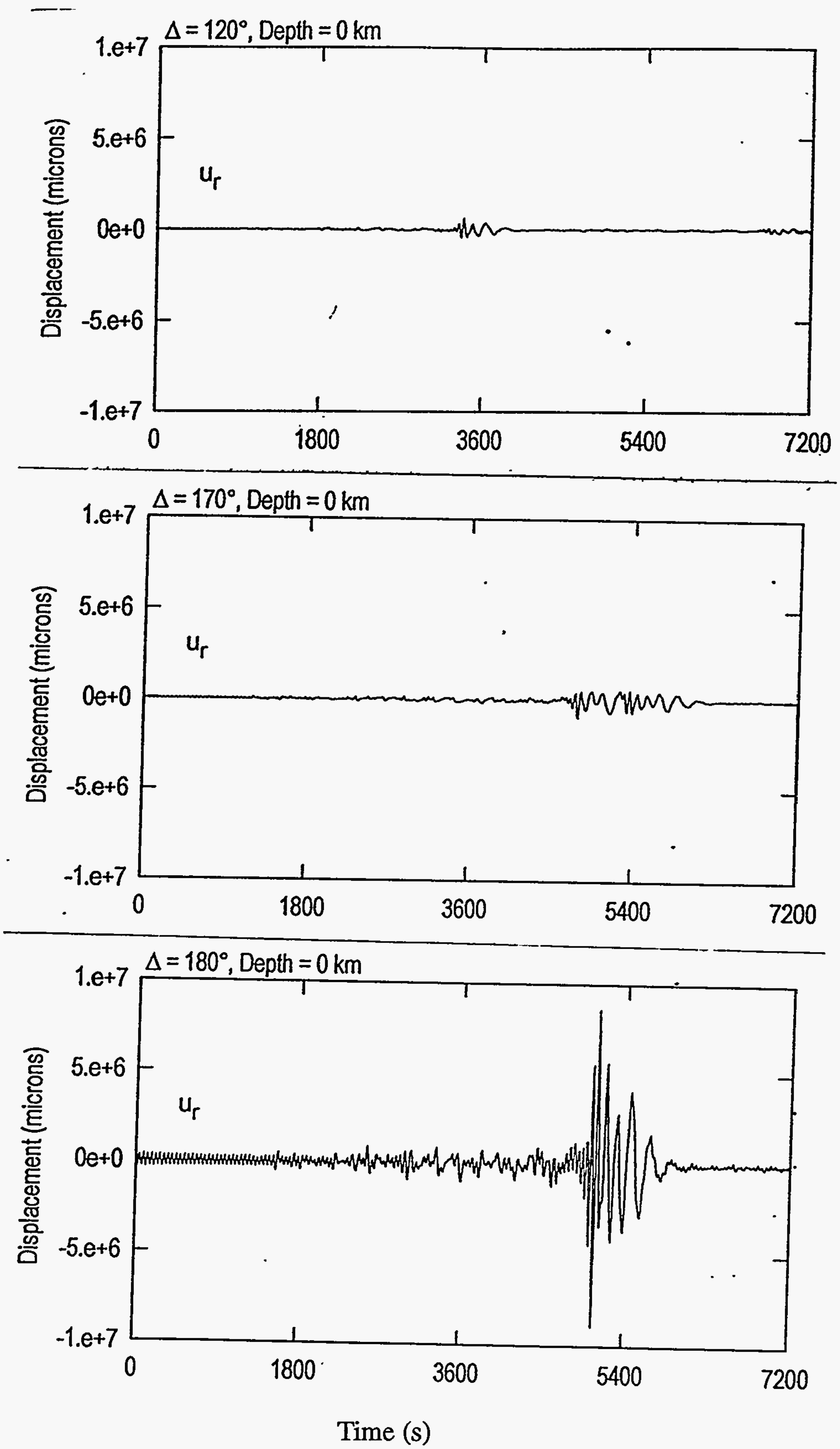

Figure 3(continued)

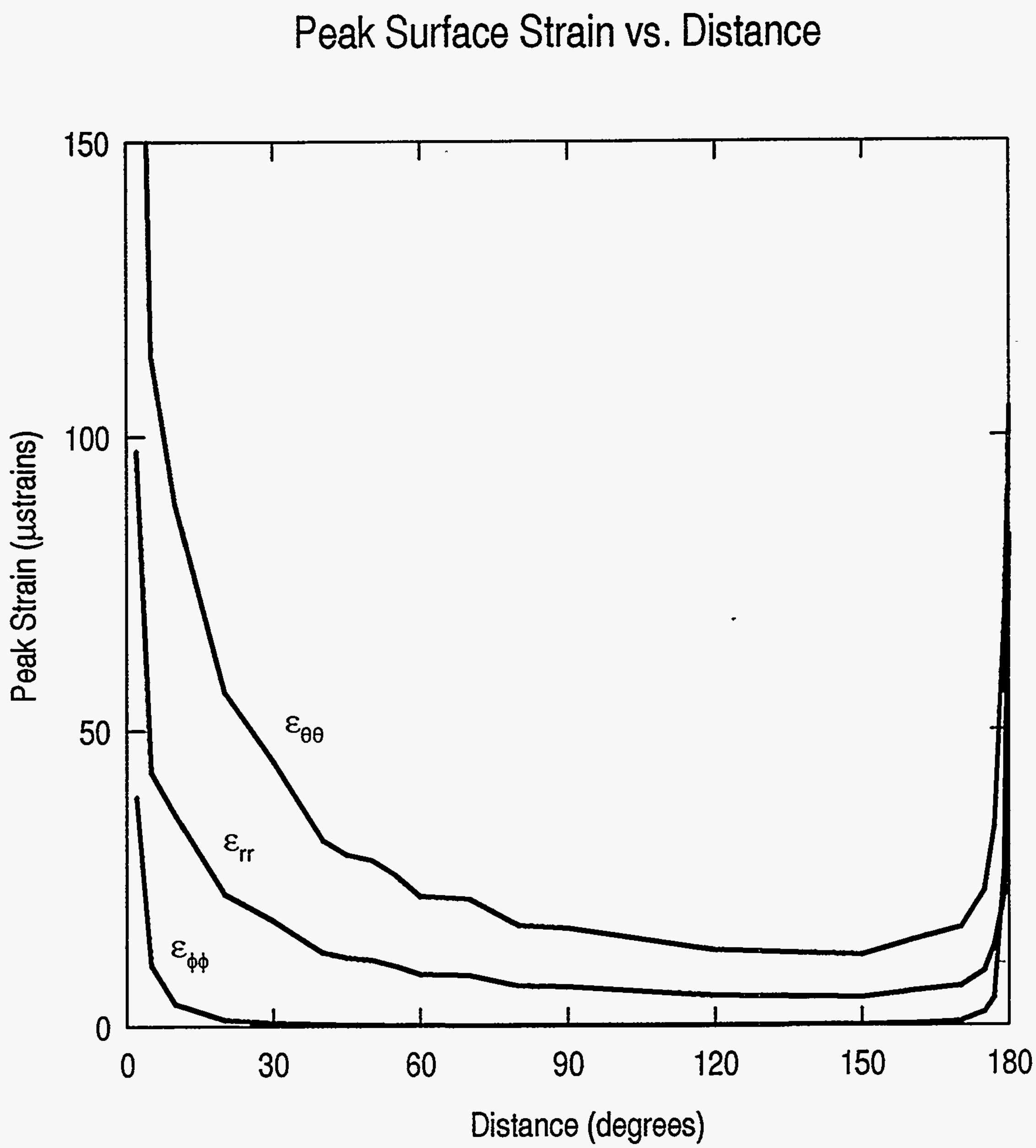
Peak Surface Strain vs. Distance
150
100
50
0
0
30
60
90
120
150
180
Peak Strain (μstrains)
Distance (degrees)
εθθ
εrr
εφφ

Figure 4

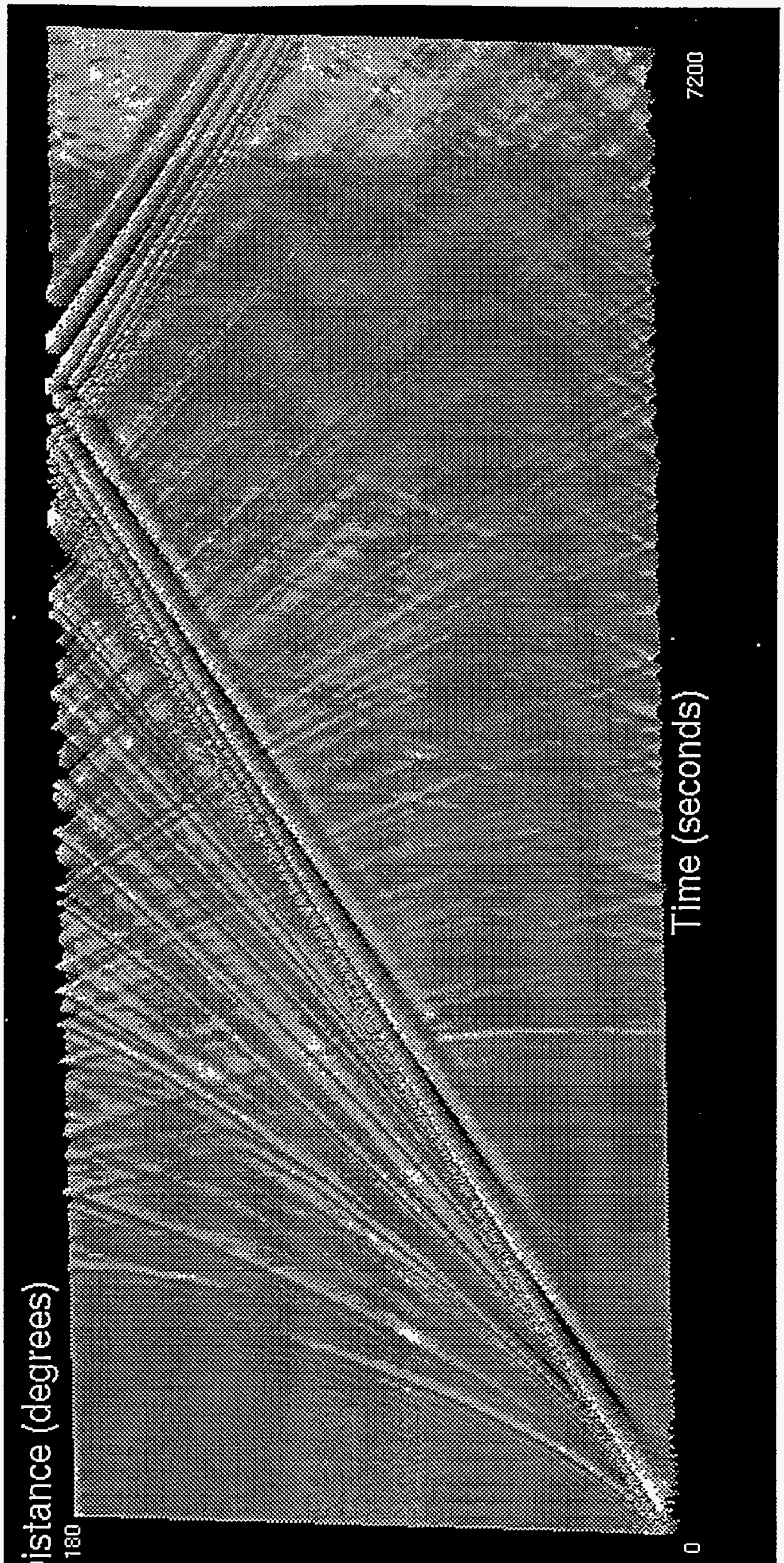

Figure 5

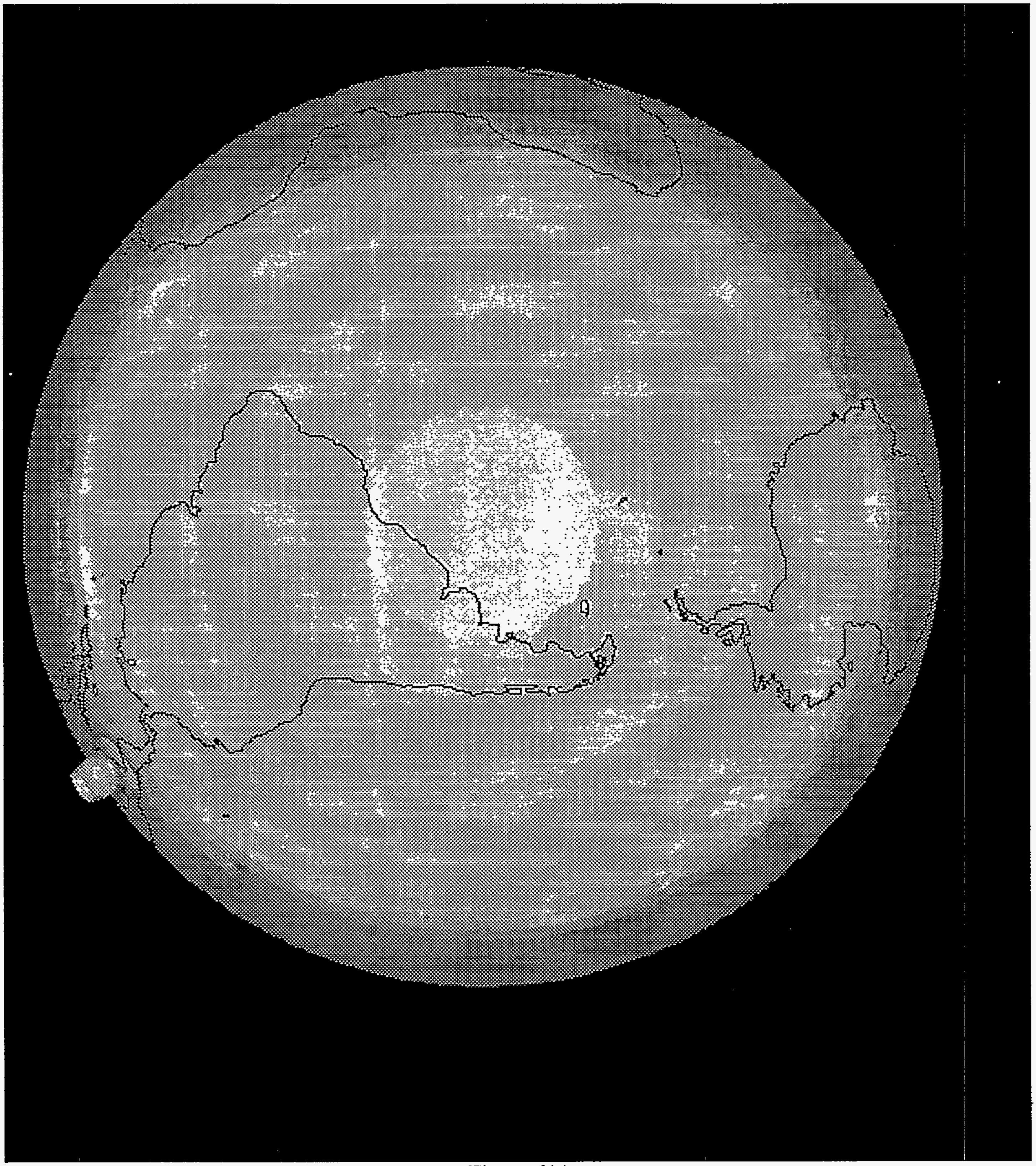

Figure 6(a)

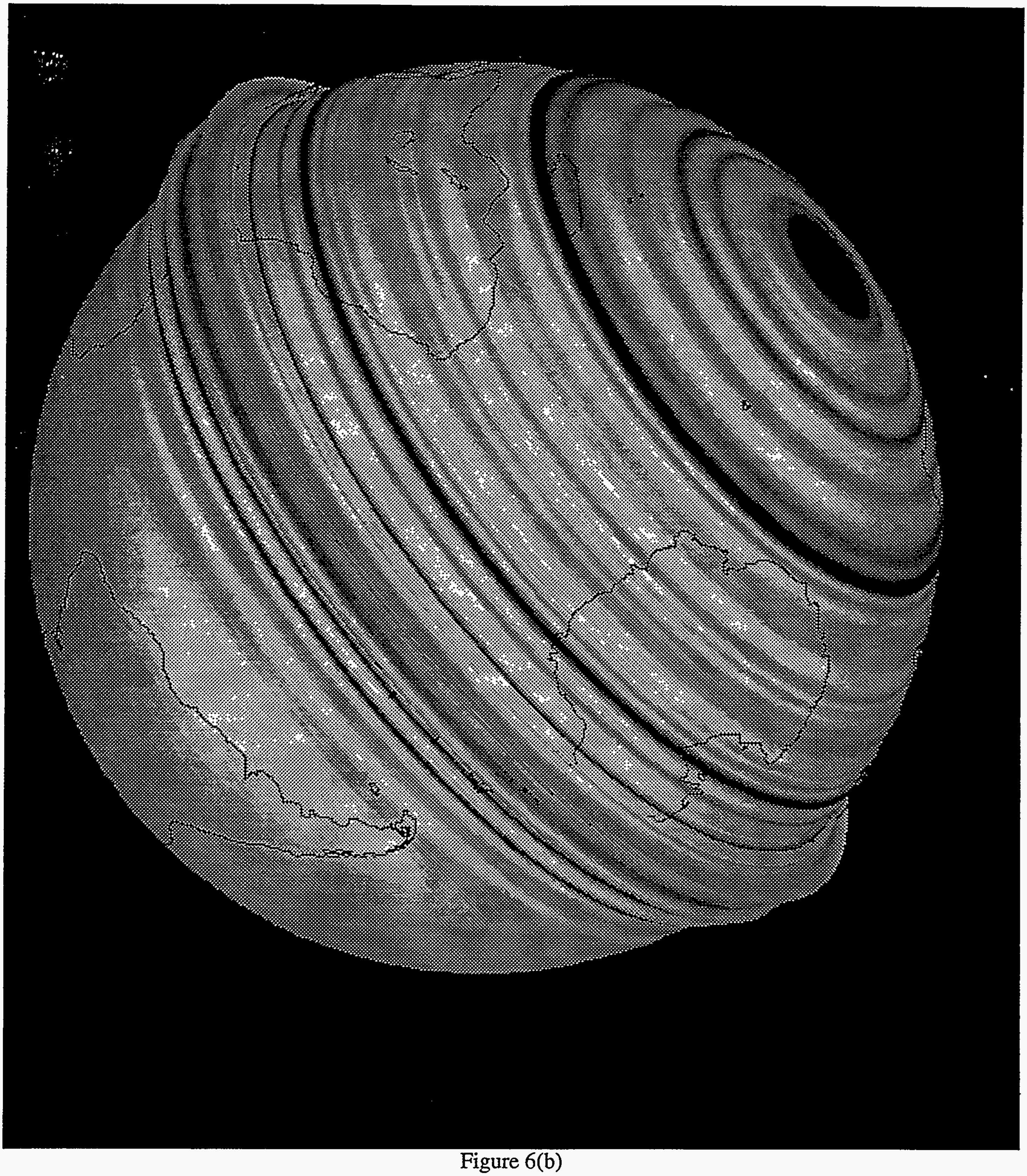
Figure 6(b)

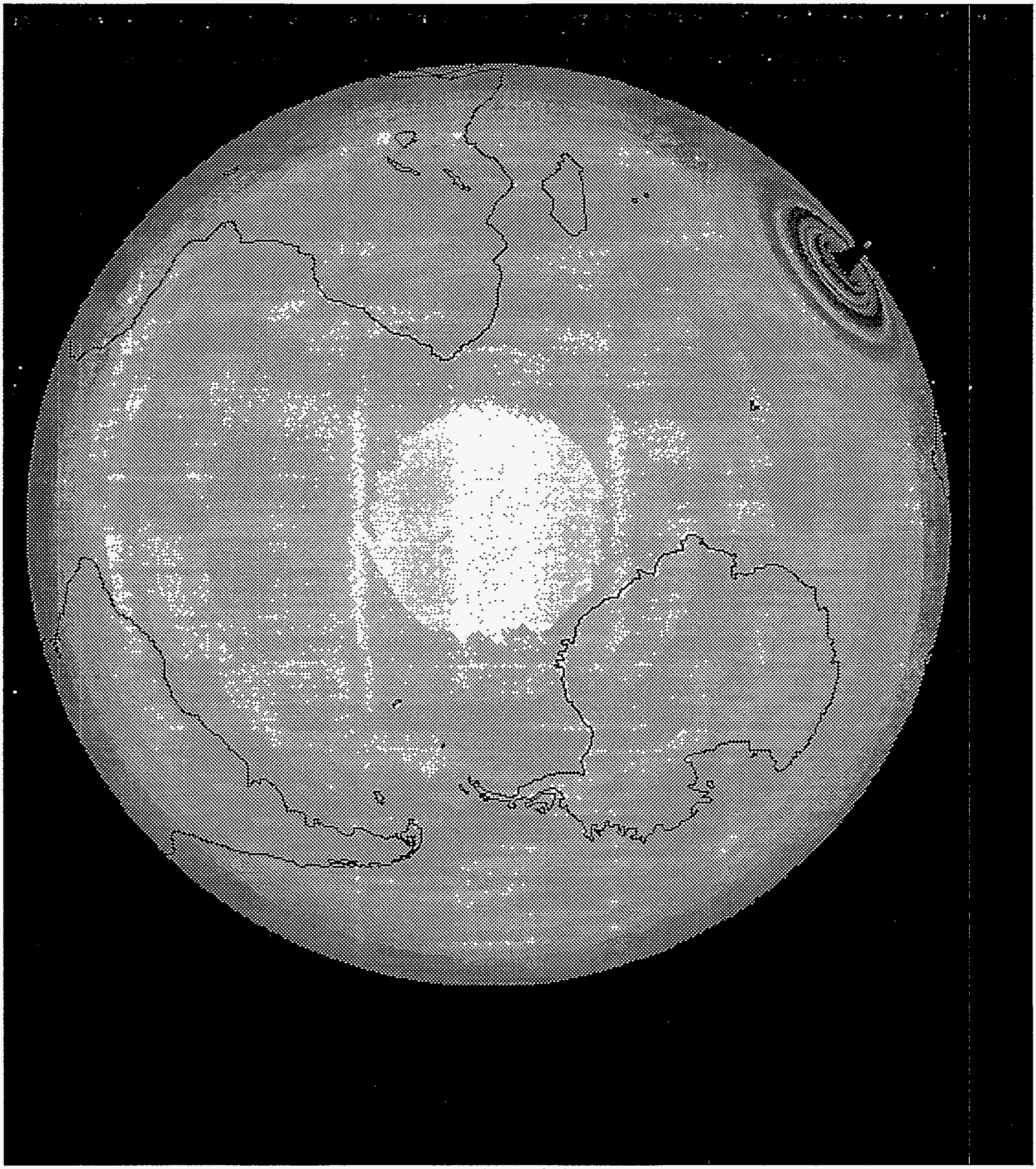

Figure 6(c)

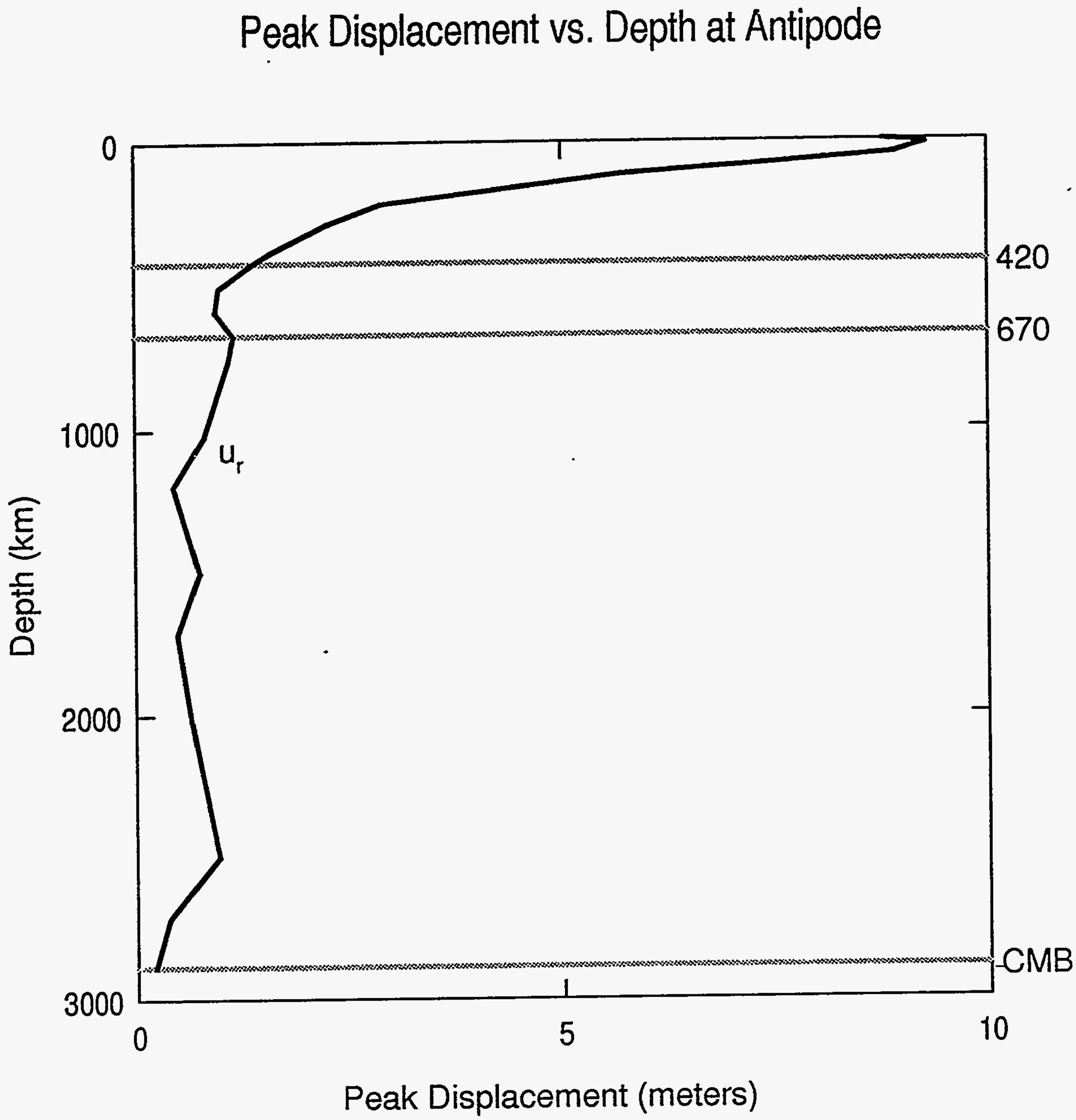

Peak Displacement vs. Depth at Antipode
0
1000
2000
3000
Depth (km)
420
670
CMB
u_r
0
5
10
Peak Displacement (meters)

Figure 7

Peak Strain vs. Depth at Antipode

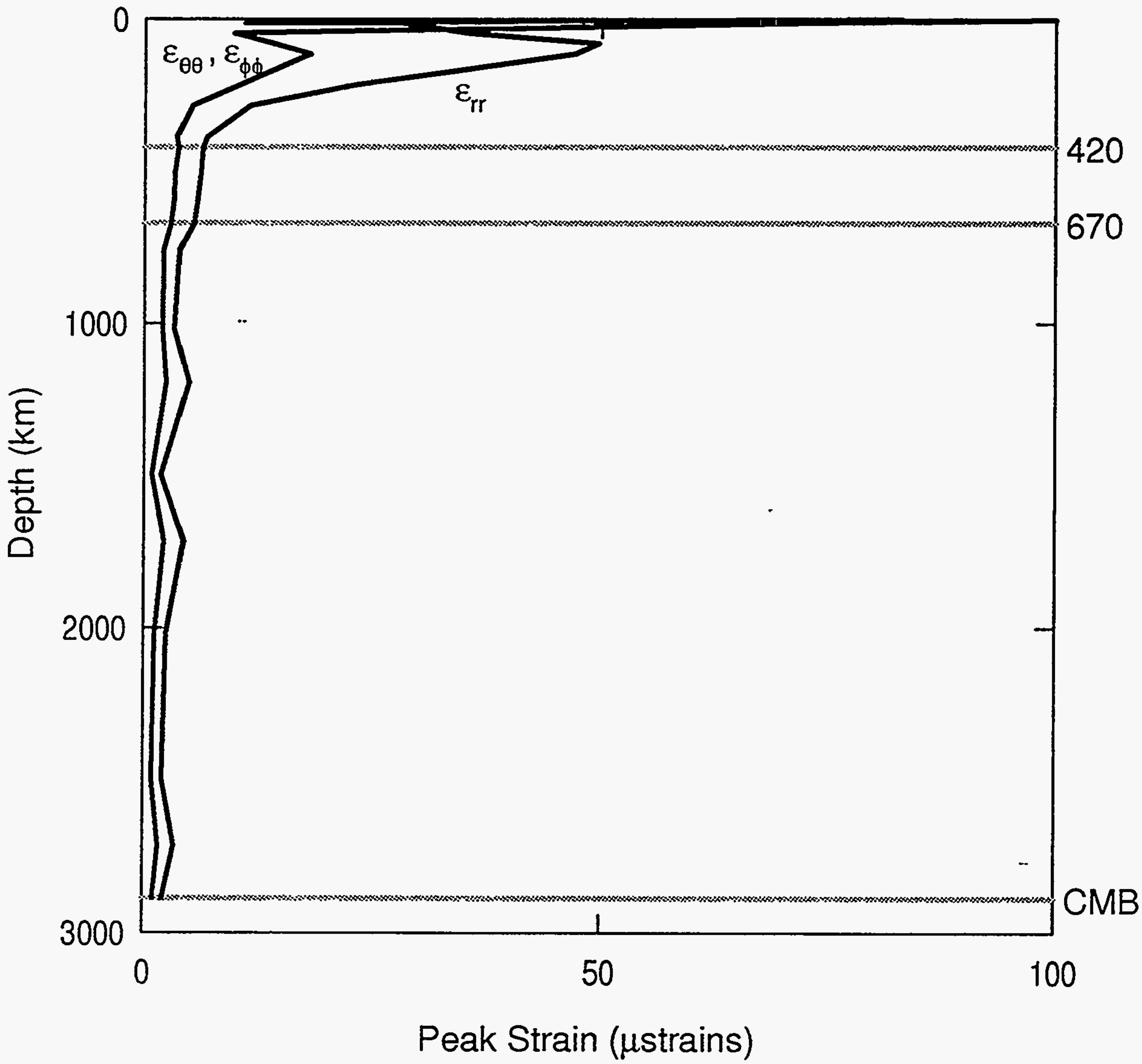

Figure 8

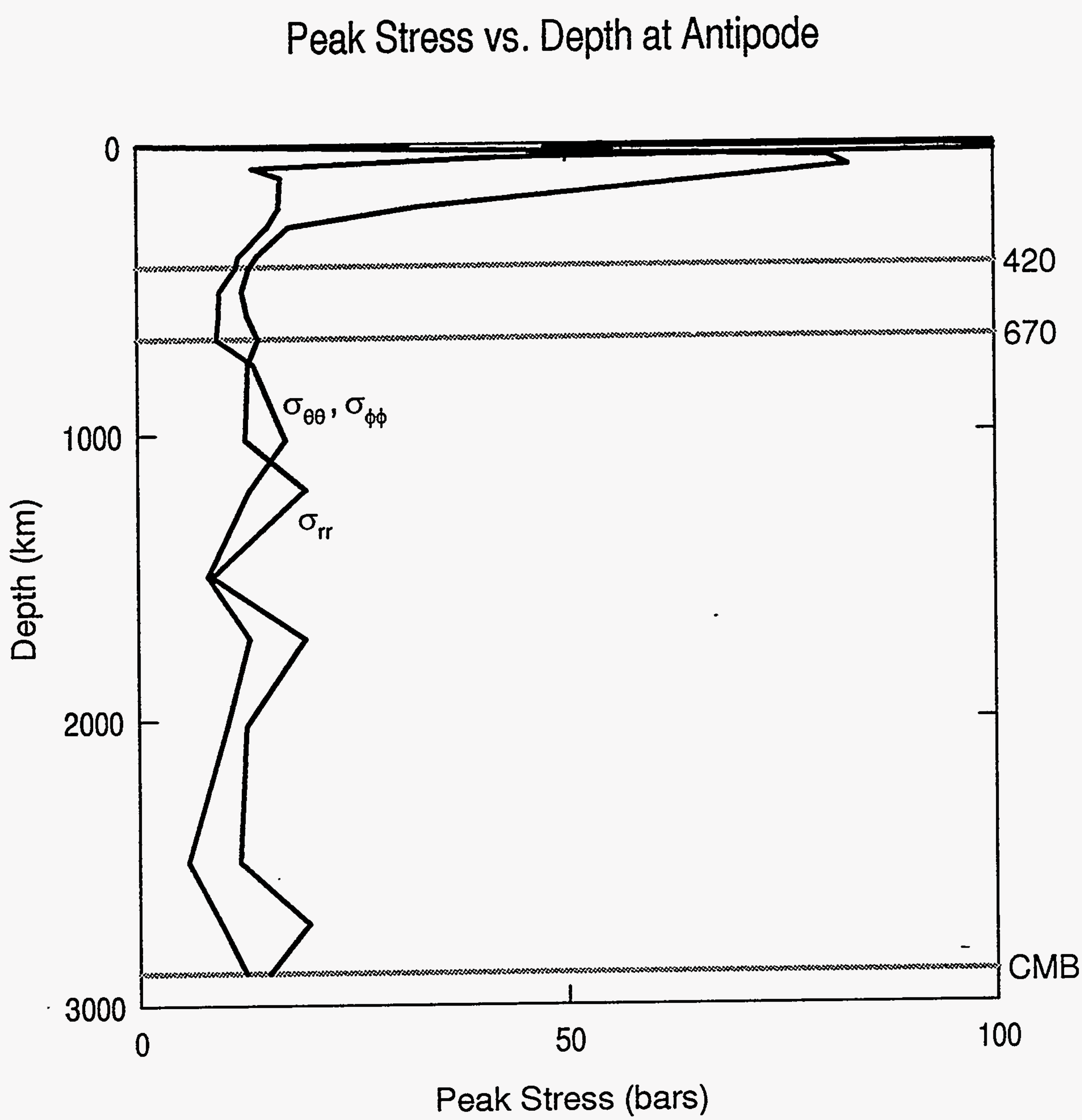
Peak Stress vs. Depth at Antipode
0
1000
2000
3000
Depth (km)
420
670
CMB
$\sigma_{\theta\theta}, \sigma_{\phi\phi}$
σ_{rr}
0
50
100
Peak Stress (bars)

Figure 9

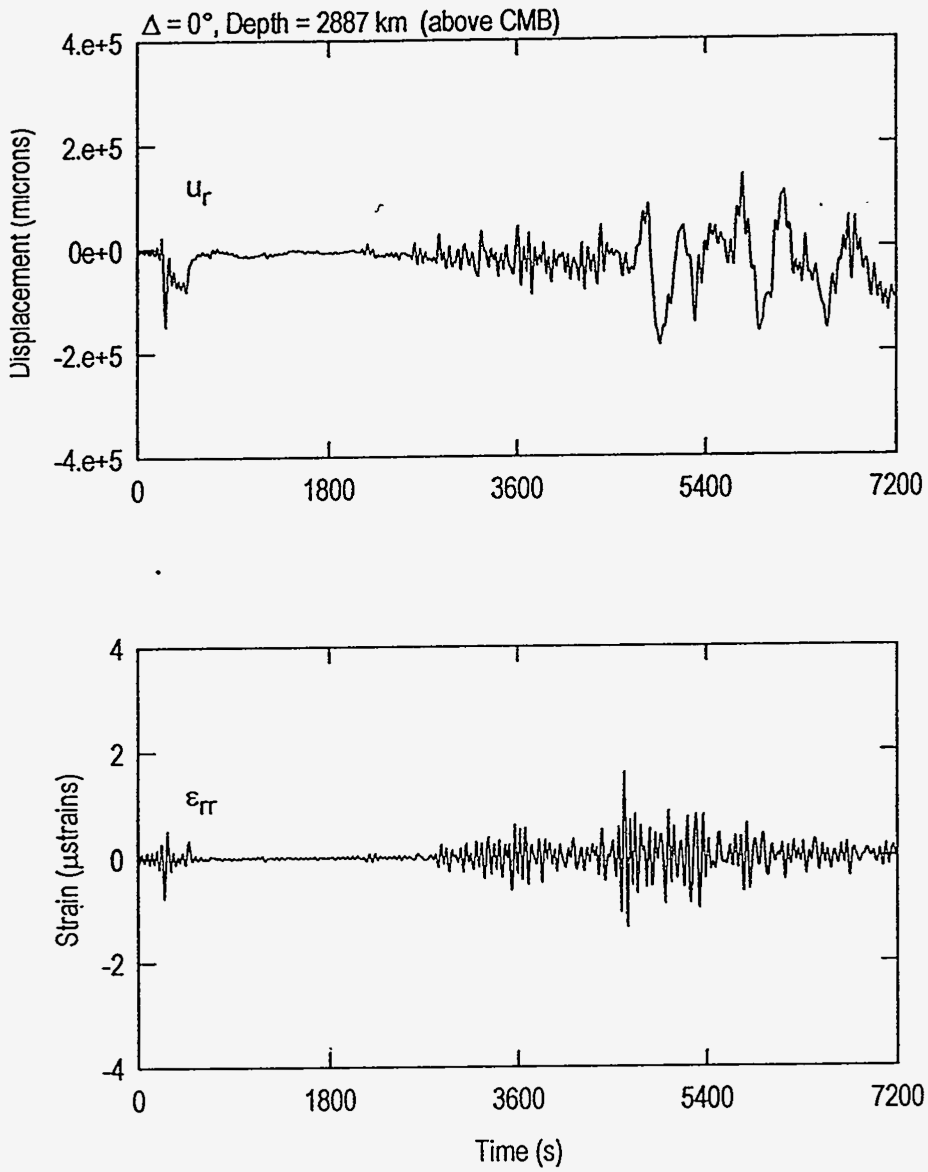
Δ = 0°, Depth = 2887 km (above CMB)
Displacement (microns)
4.e+5
2.e+5
0e+0
-2.e+5
-4.e+5
u_r
0
1800
3600
5400
7200
Strain (μstrains)
4
2
0
-2
-4
ε_rr
0
1800
3600
5400
7200
Time (s)

Figure 10a

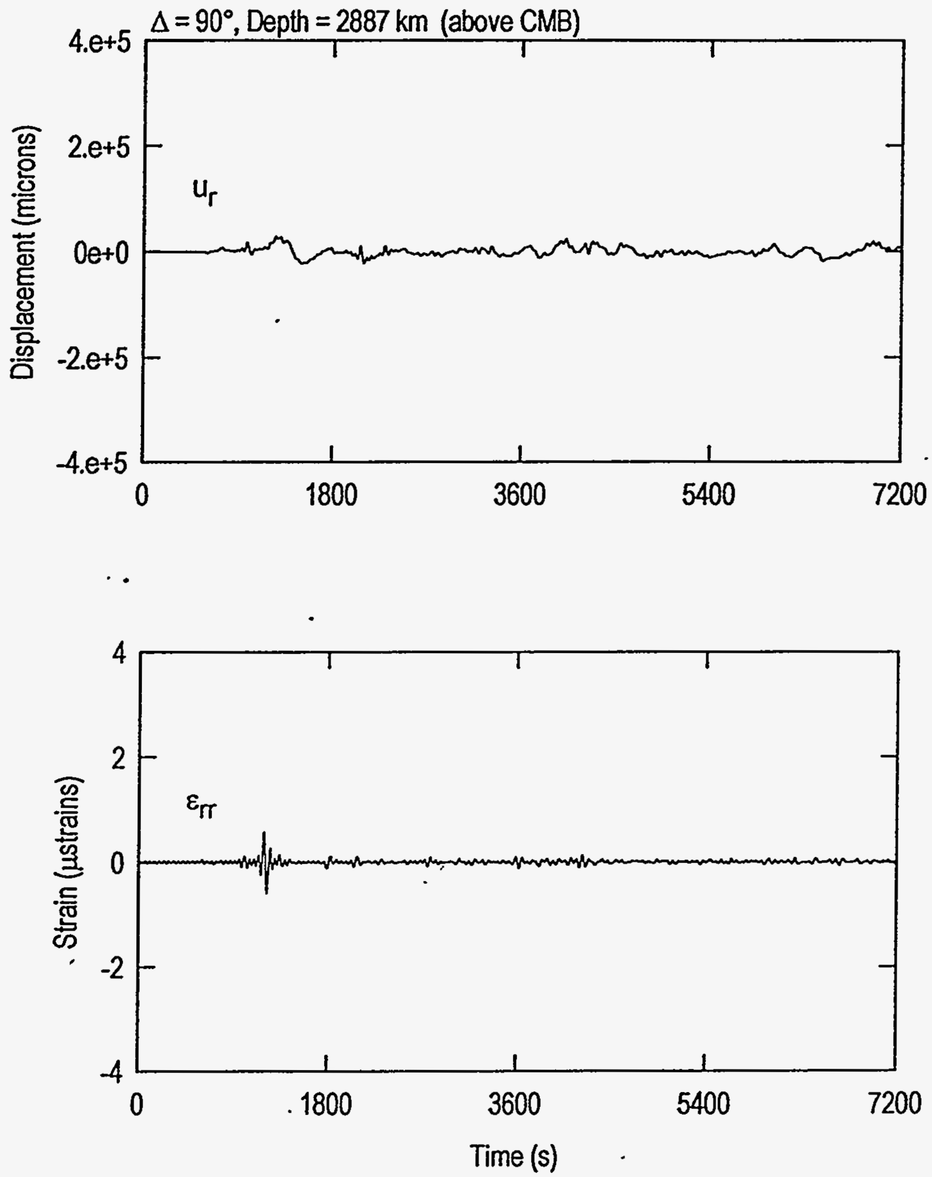

Δ = 90°, Depth = 2887 km (above CMB)
4.e+5
2.e+5
0e+0
-2.e+5
-4.e+5
Displacement (microns)
u_r
0
1800
3600
5400
7200
4
2
0
-2
-4
Strain (µstrains)
ε_rr
0
1800
3600
5400
7200
Time (s)

Figure 10b

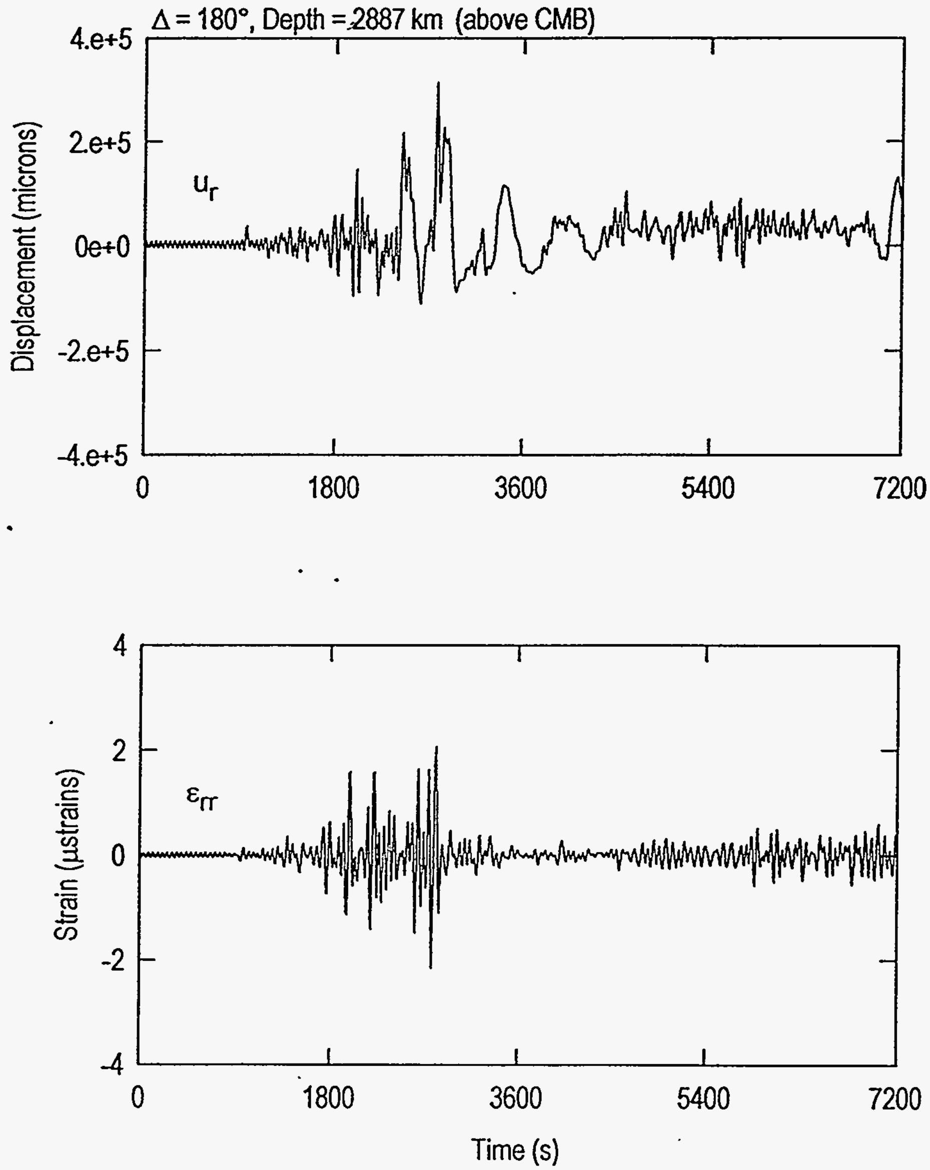
Δ = 180°, Depth = 2887 km (above CMB)
4.e+5
2.e+5
0e+0
-2.e+5
-4.e+5
Displacement (microns)
u_r
0
1800
3600
5400
7200
4
2
0
-2
-4
Strain (μstrains)
ε_rr
Time (s)

Figure 10c